**Budapest University of Technology and Economics**

**Faculty of Mechanical Engineering**

**Department of Fluid Mechanics**

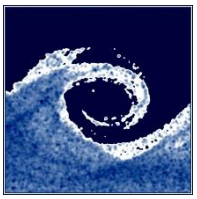

# Aerodynamic and aeroacoustic behavior of axial fan blade sections at low Reynolds numbers

*Thesis booklet of*

*Esztella Éva Balla*

*mechanical modelling engineer MSc*

*Supervisor: János VAD, DSc*

*Budapest, 2020*

# 1 Introduction and objectives

Fans are extensively used in various fields, ranging from high pressure turbofans in the aircraft industry, to ventilating or cooling fans [1], creating lower pressure rise. The family of low pressure fans represents a wide variety of rotor diameters, rotational speeds and blade geometries. Another categorization of fans is based on the direction of the outflowing air. Three types are distinguished: axial, radial and mixed flow fans. The focus of the dissertation is on axial flow fans.

The noise emission of low speed turbomachinery, including axial flow fans, has been the topic of recent research for multiple reasons. First, these machines often operate in the close vicinity of humans, making noise reduction desirable from the point of view of human comfort. Further, the emitted noise may be a symptom of losses related to aerodynamic phenomena. It is expected that by redesigning turbomachinery in order to achieve lower noise emission, the efficiency of these machines will increase besides the reduction in noise levels. Aside from the well-established use of low-speed fans in ventilating systems, a new, emerging field, where low Reynolds number turbomachinery appears, is the utilization of drones [2].

The aerodynamic and aeroacoustic behavior of fan blades has to be thoroughly examined, in order to be able to formulate design guidelines, which result in the noise reduction of fans. The aerodynamic behavior at low Reynolds numbers differs significantly from that of higher Reynolds numbers: the lift and drag coefficients of the blades become Reynolds number dependent [3, 4, 5]. As the phenomena under investigation are of great complexity, a simplified model of fan operation was taken into consideration. Single blade sections are examined, instead of full fans. The literature of such simplification in fan design is well established [3, 6].

In case of fans, aeroacoustic noise may be caused by vortex shedding from the blades [7]. One kind of vortex shedding is the so-called profile vortex shedding, which is the periodic shedding of coherent vortices over the lifting surface of the blade. Until now, the characteristic frequency at which this type of vortex shedding may occur could not be predicted by a straightforward model [7, 8, 9, 10, 11]. The author wishes to offer a method, with which the frequency can be estimated already in the design process of fans.

Larger fans, above 125 W driving motor power, have to meet certain efficiency requirements in the European Union [12]. In order to achieve better efficiency, more complex blade geometries are applied, which increases manufacturing costs. A widely used technique is the rounding of blade edges of cambered plate blades, however the effect of this rounding has not been studied in detail. If the exact aerodynamic effect of rounding is known already in the design process, then the necessity of the application of rounding can be judged. Thus the efficiency requirements may be met with a simpler geometry, saving manufacturing costs. In the dissertation an empirical model is established to judge the aerodynamic performance of cambered blades with rounded and blunt edges.

Beamforming, relying on the phased array microphone (PAM) technique, is a recently emerging methodology for obtaining spatially simultaneously resolved acoustic data on models of blade or wing sections. The usage of the phased array microphone along with the beamforming technique is increasing in the field of noise source localization. Its advantage compared to measurements

with individual microphones is that it offers a convenient way to spatially discretize the sound field. The PAM technique, as such, finds a number of turbomachinery-related applications in aerospace engineering (e.g. [13, 14, 15]). It is still, however, rare nowadays in low-speed fan-related applications (e.g. [16, 17]). The author proposes a novel measurement configuration and processing method, using the beamforming technique to localize the dominant noise, related to low-speed axial blade sections.

# 2 Results

Within this dissertation, wind tunnel measurements regarding the lift and drag force acting on various blade sections, circular-arc cambered plate blades with various cambers and a RAF6-E airfoil, are presented. The investigations were performed at Reynolds numbers between 20 000 and 140 000, and include an angle of attack range between 0° and 10°. The measurements included blades with rounded and blunt leading and trailing edges. Based on the measurement results, empirical formulae are presented for the determination of lift and drag coefficients of cambered plates, with relative cambers between 0% and 8%, angle of attack 0°-10°, and Reynolds number 40 000-140 000. The effect of bluntness of the leading and trailing edges, was also quantified. It was found that the lift coefficient decrease is 0.023 and the drag coefficient increase is 0.022, as a result of leaving the edges blunt. The above findings were summarized in Thesis statements 1 and 2.

A semi-empirical model was established for the prediction of the frequency of profile vortex shedding for various blade geometries. With the model, the third octave band, where profile vortex shedding may occur can be determined, and vortex shedding at the bands with the highest A-weight may be avoided. For the estimation of the frequency, only geometrical and operational data, and the drag coefficient is required. Compared to previous methods in the literature, the model takes into account the effect of maximum relative blade thickness and the angle of attack, and is applicable for both symmetric and non-symmetric profiles. The results are summarized in Thesis statement 3.

Measurements, involving the phased array microphone technique were conducted in order to determine the location and intensity of the noise generated by airfoils. The phased array microphone technique offers the possibility to localize the noise sources using the signals of multiple microphones. The novelty of the measurement setup is that the microphone array is placed perpendicularly to the span of the blade sections, offering the possibility to determine the location of the noise source in the chordwise and in the direction normal to the surface of the blade. One of the walls of the wind tunnel was replaced with Kevlar fabric, so that acoustic measurements could be made in a setup similar to that of the force measurements.

Dipole beamforming was applied to the microphone signals. A novel technique has been developed for the processing of phased array microphone signals as the traditional measurement technique has multiple drawbacks. Fake noise sources may appear in the noise source maps, being physically irrelevant to blade noise. Such fake sources may originate dominantly from the following circumstances. a) Measurement error related directly to the microphones. b) Background perturbations, potentially remaining even after background noise subtraction. c) Beamforming anomalies, e.g. side lobes. d) Limited spatial resolution of the phased array microphone technique, falsifying the determination of the spatial extension of the profile noise sources. The developed technique uses background subtraction, appropriate boundary conditioning and the Laplacian equation-based filtering technique, to extract useful data from the measurements, originally contaminated by perturbations. The proposed method is summarized in Thesis statement 4.

In the low-speed axial fan design the findings of the dissertation can be utilized in a practical manner. The lift and drag coefficients of blade sections can be estimated from the empirical model,

with the given uncertainties. The knowledge of lift and drag coefficients helps to identify the most suitable blade geometry for the fan. If the edges of the blade is to be kept blunt, the bluntness effect can also be taken into account in a quantified form. Additionally, an estimation can be made for the frequencies where vortex shedding may appear, already in the design phase. The phased array microphone measurements offer the possibility for the localization of the dominant profile noise, which can be utilized as background information for the reduction of fan noise.

# 3 Theses

*The literature lacks detailed aerodynamic data at Reynolds number values below $3.0 \cdot 10^5$ for cambered plates with circular arc camber line, which could be utilized in the design process of low speed axial fan bladings, and guide vanes. The aerodynamic effects of Reynolds number, angle of attack, and relative camber have been examined, in terms of lift and drag coefficients of isolated plate blade models. The studies involved wind tunnel measurements and processing of literature data. As representative cases, plates of circular-arc camber line of 0% (flat plate), 4%, 6%, and 8% were considered. The latter enables a nearly maximum lift-to-drag ratio among the cambered plates, thus offering input for blade design for high efficiency. The chord-based Reynolds numbers within $0.4 \cdot 10^5$-$3 \cdot 10^5$ were in the focus. The investigated range is below the Reynolds number of $3.0 \cdot 10^5$, for and above which aerodynamic data are available in the literature* [6]. *The angle of attack has been studied in the range of 0°-10°. This range includes states corresponding to reasonably high lift-to-drag ratio, including the angle of maximum lift-to-drag ratio for all investigated cambers. Therefore, the measurements offer data for blade design for high efficiency as well as high specific performance at moderate Reynolds numbers.*

### 1. Thesis statement

Isolated plate blades of circular arc camber line are considered, in a two-dimensional approximation. For the geometrical and operational data specified in Table T 1.1, the lift and drag coefficient values can be calculated with empirical formulae as a function of angle of attack, relative camber, and Reynolds number in the following way.

$$C_L = C_{L300} - \boldsymbol{\mathcal{S}}_L(3.00 \cdot 10^5 - Re) \qquad (T1.1)$$

$$C_D = C_{D300} - \boldsymbol{\mathcal{S}}_D(3.00 \cdot 10^5 - Re) \qquad (T1.2)$$

$C_{L300}$, $C_{D300}$, $\boldsymbol{\mathcal{S}}_L$ and $\boldsymbol{\mathcal{S}}_D$ can be estimated with the following equations:

$$C_{L300} = \sum_{i=0}^{3}\sum_{j=0}^{2} \boldsymbol{\mathcal{A}}_{ij} \left(\frac{h}{c}\right)^j \alpha^i \qquad (T1.3)$$

$$\boldsymbol{\mathcal{S}}_L = \sum_{i=0}^{3}\sum_{j=0}^{2} \boldsymbol{\mathcal{B}}_{ij} \left(\frac{h}{c}\right)^j \alpha^i \qquad (T1.4)$$

$$C_{D300} = \sum_{i=0}^{3}\sum_{j=0}^{2} \boldsymbol{\mathcal{C}}_{ij} \left(\frac{h}{c}\right)^j \alpha^i \qquad (T1.5)$$

$$\boldsymbol{\mathcal{S}}_D = \sum_{i=0}^{3}\sum_{j=0}^{2} \boldsymbol{\mathcal{D}}_{ij} \left(\frac{h}{c}\right)^j \alpha^i \qquad (T1.6)$$

$h/c$ is in percent and $\alpha$ is in degrees. The values of the empirical coefficients are summarized in Table T 1.2, Table T 1.3, Table T 1.4 and Table T 1.5. The overall precision of the model, described with the uncorrected standard deviation is ±3% for $C_L$ and ±8% for $C_D$. The symbols are explained in Table T 1.6.

*Table T 1.1 Geometrical and operational data*

| | |
|---|---|
| *h/c* | 0% - 8% |
| *t/c* | 2% - 3% |
| *Re* | $0.4 \cdot 10^5$ - $3.0 \cdot 10^5$ |
| $\alpha$ | 0° - 10° |
| Leading and trailing edge layout | Rounded |

*Table T 1.2 Empirical coefficients for the datum point of the lift coefficient*

| | | i | | | |
|---|---|---|---|---|---|
| | $\mathcal{A}$ | 0 | 1 | 2 | 3 |
| j | 0 | $-8.20 \cdot 10^{-3}$ | $3.85 \cdot 10^{-2}$ | $2.25 \cdot 10^{-2}$ | $-1.87 \cdot 10^{-3}$ |
| | 1 | $1.04 \cdot 10^{-1}$ | $2.76 \cdot 10^{-2}$ | $-7.99 \cdot 10^{-3}$ | $5.57 \cdot 10^{-4}$ |
| | 2 | $-4.25 \cdot 10^{-4}$ | $-2.66 \cdot 10^{-3}$ | $6.22 \cdot 10^{-4}$ | $-4.06 \cdot 10^{-5}$ |

*Table T 1.3 Empirical coefficients for the slope of the lift coefficient*

| | | i | | | |
|---|---|---|---|---|---|
| | $\mathcal{B}$ | 0 | 1 | 2 | 3 |
| j | 0 | $5.78 \cdot 10^{-7}$ | $-5.82 \cdot 10^{-7}$ | $1.59 \cdot 10^{-7}$ | $-1.08 \cdot 10^{-8}$ |
| | 1 | $-2.07 \cdot 10^{-7}$ | $2.79 \cdot 10^{-7}$ | $-5.74 \cdot 10^{-8}$ | $3.50 \cdot 10^{-9}$ |
| | 2 | $4.44 \cdot 10^{-8}$ | $-2.93 \cdot 10^{-8}$ | $5.08 \cdot 10^{-9}$ | $-2.84 \cdot 10^{-10}$ |

*Table T 1.4 Empirical coefficients for the datum point of the drag coefficient*

| | | i | | | |
|---|---|---|---|---|---|
| | $\mathcal{C}$ | 0 | 1 | 2 | 3 |
| j | 0 | $1.34 \cdot 10^{-2}$ | $-1.98 \cdot 10^{-3}$ | $1.84 \cdot 10^{-3}$ | $-1.10 \cdot 10^{-5}$ |
| | 1 | $3.50 \cdot 10^{-3}$ | $-2.49 \cdot 10^{-4}$ | $-7.35 \cdot 10^{-4}$ | $4.53 \cdot 10^{-5}$ |
| | 2 | $-2.27 \cdot 10^{-4}$ | $-1.49 \cdot 10^{-5}$ | $7.61 \cdot 10^{-5}$ | $-5.44 \cdot 10^{-6}$ |

*Table T 1.5 Empirical coefficients for the slope of the drag coefficient*

| | | i | | | |
|---|---|---|---|---|---|
| | $\mathcal{D}$ | 0 | 1 | 2 | 3 |
| j | 0 | $3.29 \cdot 10^{-8}$ | $-6.38 \cdot 10^{-8}$ | $5.76 \cdot 10^{-9}$ | $4.54 \cdot 10^{-12}$ |
| | 1 | $-1.37 \cdot 10^{-8}$ | $2.61 \cdot 10^{-8}$ | $-4.90 \cdot 10^{-9}$ | $9.73 \cdot 10^{-11}$ |
| | 2 | $-7.39 \cdot 10^{-10}$ | $-2.65 \cdot 10^{-9}$ | $5.30 \cdot 10^{-10}$ | $-1.30 \cdot 10^{-11}$ |

*Table T 1.6 List of symbols*

| | |
|---|---|
| $\mathcal{A}, \mathcal{B}, \mathcal{C}, \mathcal{D}$ | empirical coefficients [-] |
| $c$ | chord [m] |
| $C_D$ | drag coefficient [-] |
| $C_L$ | lift coefficient [-] |
| $C_{D300}$ | drag coefficient datum point [-] |
| $C_{L300}$ | lift coefficient datum point [-] |
| $h$ | maximum height of the camber line [m] |
| $i,j$ | indices |
| $\mathcal{S}_D$ | drag coefficient slope [-] |
| $\mathcal{S}_L$ | lift coefficient slope [-] |
| $Re$ | chord based Reynolds number [-] |
| $t$ | maximum blade thickness [m] |
| $\alpha$ | angle of attack [°] |

Related publications: [P1][P2][P3][P4]

*For simplification in manufacturing of plate blades of axial fans, the blade leading and trailing edges are occasionally left blunt. For blade design considerations, the aerodynamic effects of leading and trailing edge bluntness have been examined, in terms of lift and drag coefficients of isolated plate blade models. The studies involved wind tunnel measurements and processing of literature data. As representative cases, plates of circular-arc camber line of 0% (flat plate), 4%, and 8% were considered. The chord-based Reynolds numbers within $4.0 \cdot 10^4$-$1.4 \cdot 10^5$ were in the focus. The angle of attack has been studied in the range of 0°-10°. The expected change in the lift and drag coefficients due to leaving the edges blunt, as well as the uncorrected standard deviation of the change has been determined. $\Delta C_L$ and $\Delta C_D$ are defined as the difference between the lift/drag coefficient of the rounded case and the lift/drag coefficient of the blunt case. The adverse effect of edge bluntness on $C_L$ and $C_D$ was quantified, using single-value metrics in a conservative manner, in the following way. The decrease in $C_L$ due to edge bluntness is the expected value of $\Delta C_L$ minus the uncorrected standard deviation of $\Delta C_L$. The increase in $C_D$ due to edge bluntness is the expected value of $\Delta C_D$ plus the uncorrected standard deviation of $\Delta C_D$.*

## 2. Thesis statement

Isolated plate blades of circular arc camber line are considered. For the geometrical and operational data specified in Table T 2.1, leaving the blade leading and trailing edge blunt causes the following departure in the aerodynamic properties, in comparison to reference cases incorporating rounded edge layout:

- $C_L$: decrease by 0.023
- $C_D$: increase by 0.022

The symbols are explained in Table T 2.2.

*Table T 2.1 Geometrical and operational data*

| | |
|---|---|
| *h/c* | 0%-8% |
| *t/c* | 2% - 3% |
| *Re* | $4.0 \cdot 10^4$-$1.4 \cdot 10^5$ |
| *α* | 0°-10° |

*Table T 2.2 List of symbols*

| | |
|---|---|
| $c$ | chord [m] |
| $C_D$ | drag coefficient [-] |
| $C_L$ | lift coefficient [-] |
| $h$ | maximum height of the camber line [m] |
| $Re$ | chord based Reynolds number [-] |
| $t$ | maximum blade thickness [m] |
| $\alpha$ | angle of attack [°] |
| $\Delta C_D$ | drag coefficient difference between the case with rounded and blunt leading edge [-] |
| $\Delta C_L$ | lift coefficient difference between the case with rounded and blunt leading edge [-] |

Related publication: [P1][P2][P3][P4]

*Prediction of profile vortex shedding frequency in blade design is of practical importance, since profile vortex shedding represents a risk from a blade vibration, as well as from noise emission point of view. For the judgement of these unfavorable effects, the third-octave frequency band affected by profile vortex shedding is to be determined. The studies involved hot-wire measurements and processing of literature data. Profiles of 2%-25% maximum thickness-to-chord ratio, and with and without camber were considered. The chord-based Reynolds numbers within $0.5 \cdot 10^5$-$15 \cdot 10^5$ were in the focus, including the range of low-speed axial fans. The angle of attack has been studied in the range of 0°-10°. The model utilizes the universal Strouhal number, defined in* [18]*, its value being St* = 0.16 for the investigated cases. Compared to the recommendations available in the literature, the proposed model takes into account the different geometries and operating conditions by introducing the maximum relative blade thickness and angle of attack dependency. Additionally, instead of the boundary layer thickness, which is uncertain to determine due to the complexity of fan rotors, the model uses an integral-based parameter, the wake momentum thickness. The value of the wake momentum thickness is obtainable from the drag if direct measurements are unavailable. With the above supplementation, the model offers an estimation of profile vortex shedding frequency, for a wide variety of profile geometries and angles of attack.*

## 3. Thesis statement

Isolated blades are considered. For the geometrical and operational data specified in Table T 3.1, the base frequency at which profile vortex shedding may occur, can be estimated as

$$f = \frac{b}{U_0 \, St^*} \qquad (T3.1)$$

The value of the universal Strouhal number is $St^*$=0.16.

$b$ can be calculated as

$$b = K^* \theta \qquad (T3.2)$$

$K^*$ can be determined with the following empirical equation:

$$K^* = 1.9 + 0.19\frac{t}{c} - 0.023\alpha_L^2 \qquad (T3.3)$$

where $\alpha_L$ is the angle of attack in degrees, $\alpha_L$ = 0° corresponds to the angle of zero lift, shown in Figure T 3.1.

$\theta$ is to be determined from the drag coefficient, $C_D$ in the following way

$$\theta = c\frac{C_D}{2} \qquad (T3.4)$$

The schematic of the whole model is shown in Figure T 3.2. The overall precision of the model, described with the uncorrected standard deviation is ±27% for $K^*$ and ±30% for $f$. The symbols are explained in Table T 3.2.

*Table T 3.1 Geometrical and operational data*

| | |
|---|---|
| *t/c* | 2%-25% |
| *Re* | $0.5 \cdot 10^5$-$15 \cdot 10^5$ |
| $\alpha_L$ | 0°-10° |

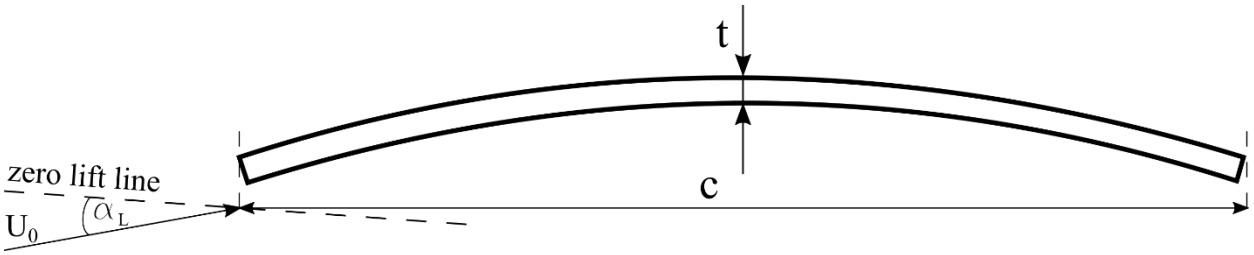


*Figure T 3.1 Sketch of a profile with indication of characteristic quantities*

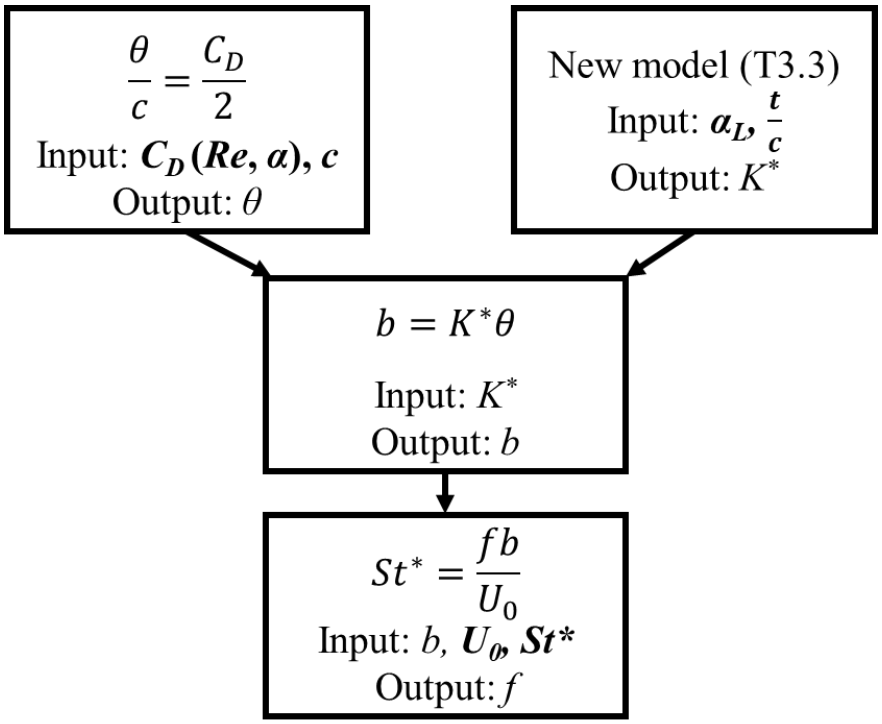


*Figure T 3.2 Flowchart presenting the process of profile vortex shedding frequency estimation. The independent input parameters are in bold*

*Table T 3.2 List of symbols*

| | |
|---|---|
| $b$ | transversal distance between vortex rows [m] |
| $c$ | chord [m] |
| $C_D$ | drag coefficient [-] |
| $f$ | frequency of vortex shedding [Hz] |
| $K^*$ | momentum thickness based frequency scaling factor [-] |
| $St^*$ | universal Strouhal number[-] |
| $t$ | maximum relative blade thickness [m] |
| $U_0$ | free-stream velocity [m/s] |
| $\alpha_L$ | zero lift based angle of attack [°] |
| $\theta$ | wake momentum thickness [m] |

Related publications: [P5] [P6]

*The identification of the dominant source of profile noise was the aim of the investigations. The localization is necessary in the chordwise direction, and in the direction normal to the blade surface. The studies involved phased array microphone measurements on models of axial fan blade sections, from an observation plane perpendicular to the span of the profiles. The measurements were carried out in a wind tunnel originally designed for aerodynamic measurements. The measurement data is processed with a novel Laplacian equation-based filtering technique, in order to obtain relevant results from the measurements highly contaminated with perturbations. The three investigated profile geometries included a flat plate, a cambered plate and a RAF6-E profile. The flat plate serves as a reference case, while the cambered plate and the RAF6-E are representative examples of blade geometries used in low-speed axial fan or guide vane design. The chord-based Reynolds numbers within $0.6 \cdot 10^5$-$1.4 \cdot 10^5$ were in the focus, representing the operating range of low-speed axial fans. The angle of attack has been studied in the range of 0°-6°. The proposed processing method offers the possibility to localize the dominant sources of profile noise, from measurements made in a wind tunnel lacking special aeroacoustic treatment.*

## 4. Thesis statement

The dominant noise peak related to the noise of an isolated rectilinear airfoil can be localized in the chordwise direction, and in the direction normal to the chord and span, with a Phased Array Microphone (PAM), in a wind tunnel, using the following method. The symbols are explained in Table T 4.1.

- The airfoil is placed in a wind tunnel, which is closed at the two tips of the airfoil. One wall is made of Kevlar fabric.
- Planar PAM is applied. The plane of the PAM is placed perpendicular to the span of the airfoil.
- PAM measurement pairs are created, containing a measurement at presence, and a measurement in absence of the airfoil. To achieve this, sound is recorded at the desired airfoil configurations, and also at an empty, running wind tunnel at the desired flow speeds.
- Beamforming is applied to the recorded microphone signals.
- Background subtraction is applied the following way:

$$SS_U(x,z) = SS_W(x,z) - SS_{BG}(x,z) \qquad (T4.1)$$

- A confinement of rectangular Region of Interest (ROI) surrounding the airfoil, resulting in $ROI_F$, is used to enrich the useful information in the signal. The confinement of ROI is to meet the following requirements:
  1. $\overline{SS}_U$ is to be positive
  2. $\overline{SS}_U$ is to increase as $A_{ROI}$ decreases in the $A_{ROI}$ range neighboring $ROI_F$
  3. $P$ is to degressively increase as $A_{ROI}$ increases in the $A_{ROI}$ range neighboring $ROI_F$

  where

$$\overline{SS}_U = \frac{\int_{A_{ROI,F}} SS_U(x,z)dA}{A_{ROI,F}} \quad (T4.2)$$

$$P = \overline{SS}_U \cdot A_{ROI} \quad (T4.3)$$

- Constant value is to be prescribed on the boundary of the investigated domain according to the following equation:

$$SS_{boundary} := \frac{\int_{A_{ROI,F}} SS_U(x,z)dA}{A_{ROI,F}} \quad (T4.4)$$

- A target intensity amplitude value is to be determined in the following way:

$$C_{PSF} = \frac{\int_{A_{ROI,F}} [SS_U - SS_{U,min}](x,z)dA}{\int_{A_{ROI,F}} PSF_n(x,z)dA} \quad (T4.5)$$

- Laplacian equation-based filtering is to be performed on the $ROI_F$ grid in a discretized way, evolving from the rectangular ROI boundary toward the chordline of the airfoil:

$$SS_k(x_i,z_i) := \frac{1}{4}\{SS_{k-1}(x_i+\Delta d,z_i) + SS_{k-1}(x_i-\Delta d,z_i) + SS_{k-1}(x_i,z_i+\Delta d) + \\ + SS_{k-1}(x_i,z_i-\Delta d)\} \quad (T4.6)$$

  The Laplacian equation-based filtering should be carried out multiple times, until the intensity level of the peak becomes equal to $C_{PSF} + SS_{U,min}$.

The output of the above method is the location and the $C_{PSF} + SS_{U,min}$ amplitude of a single dominant point source.

*Table T 4.1 List of symbols*

| | |
|---|---|
| $A_{ROI,F}$ | area of the spatially confined region [$m^2$] |
| $C_{PSF}$ | target intensity amplitude [$Pa^2$] |
| $\Delta d$ | spacing of the computational grid of the spatially confined region [m] |
| $P$ | *SS* integrated on a surface, analogous quantity with sound power [$Pa^2m^2$] |
| $PSF_n$ | normalized point spread function at the investigated frequency [-] |
| $ROI_F$ | rectangular spatial confinement, region of interest |
| $SS_{boundary}$ | source strength on the boundary of the spatially confined region [$Pa^2$] |
| $SS_{BG}$ | source strength normalized by a reference value, when the wind tunnel was empty [$Pa^2$] |
| $SS_k$ | Laplace equation-based filtered source strength, for k cycles[$Pa^2$] |
| $SS_U$ | unfiltered source intensity after background subtraction [$Pa^2$] |
| $\overline{SS}_U$ | area-averaged source intensity related to the profile [$Pa^2$] |
| $SS_{u,min}$ | minimum of the $SS_U$ [$Pa^2$] |
| $SS_W$ | source strength normalized by a reference value, for the measurements when an airfoil was present in the wind tunnel [$Pa^2$] |
| $x$ | spatial coordinate in the streamwise direction [m] |
| $z$ | spatial coordinate in the transversal direction [m] |

Related publications: [P7][P8][P9][P10]

# The author's publications related to the thesis


[P1] E. Balla and J. Vad, "An empirical model to determine lift and drag coefficients of cambered plates at moderate Reynolds numbers," *Proceedings of the Institution of Mechanical Engineers, Part A: Journal of Power and Energy,* Online first, 2020.

[P2] B. Nagy and E. Balla, "Szárnymetszetek körüli áramlás szimulációja alacsony Reynolds-számokon," in *Proceedings of Spring Wind 2017 International Multidisciplinary Conference*, Miskolc, Hungary, pp. 90-101, 31 March-02 April 2017

[P3] E. Balla, "Numerical simulations on basic models of low-speed axial fan blade sections," in *Proceedings of the 6th International Scientific Conference on Advances in Mechanical Engineering (ISCAME 2018) : Book of extended abstracts*, Debrecen, Hungary, pp. 9-10, 11-12 October 2018

[P4] E. Balla and J. Vad, "Lift and drag force measurements on basic models of low-speed axial fan blade sections," *Proceedings of the Institution of Mechanical Engineers, Part A: Journal of Power and Energy,* vol. 233, no. 2, pp. 165-175, 2019.

[P5] E. Balla and J. Vad, "A semi-empirical modell for predicting the frequency of profile vortex shedding relevant to low-speed axial fan blade sections," in *The 13th European Conference on Turbomachinery Fluid Dynamics and Thermodynamics*, Lausanne, Switzerland, Paper ID: 311, 12p., 8-12 April 2019.

[P6] E. Balla, "Lapátmetszetek körüli áramlás által keltett zaj szimulációs vizsgálata," in *Proceedings of Spring Wind 2018 International Multidisciplinary Conference*, Győr, Hungary, pp. 30-38, 04-06 May 2018

[P7] E. Balla and J. Vad, "Establishment of a beamforming dataset on basic models of low-speed axial fan blade sections," *Periodica Polytechnica, Mechanical Engineering,* vol. 61, no. 2, pp. 122-129, 2017.

[P8] E. Balla and J. Vad, "Combined aerodynamic and phased array microphone studies on basic models of low-speed axial fan blade sections," in *ASME Turbo Expo 2018: Turbomachinery Technical Conference and Exposition*, Oslo, Norway, Paper ID: GT2018-75778, p. 11, 11-15 June 2018.

[P9] E. Balla and J. Vad, "Beamforming studies on basic models of low-speed axial fan blade sections," in *Proceedings 12th European Conference on Turbomachinery Fluid Dynamics and Thermodynamics (ETC'12)*, Stockholm, Sweden, Paper ID: ETC2017-119, p. 13, 3-7 April 2017.

[P10] E. Balla and J. Vad, "A Laplacian filtering-based technique to localize vortex shedding noise in a strongly contaminated environment", *8th Berlin Beamforming Conference*, Berlin, Germany, Paper ID: BeBeC-2020-D12, p. 19, 2-3 March 2020.

# References


[1] L. X. Huang, "Characterizing computer cooling fan noise," *The Journal of the Acoustical Society of America,* vol. 114, pp. 3189-3200, 2003.

[2] T. J. Mueller, "Aerodynamic measurements at low Reynolds numbers for fixed wing micro-air vehicles," in *RTO AVT/VKI Special Course, Development and operation of UAVs for military and civil applications,* VKI, Belgium, 13-17 September 1999.

[3] T. Carolus, Ventilatoren, Wiesbaden: B. G. Teubner Verlag, 2003.

[4] W. Albring, Angewandte Strömungslehre, 6th ed., Berlin: Akademie-Verlag, 1990.

[5] J. McMasters and M. Henderson, "Low-speed single-element airfoil synthesis," *Technical Soaring,* vol. 6, no. 2, p. 1–21, 1980.

[6] R. A. Wallis, Axial flow fans, London: George Newnes Ltd., 1961.

[7] H. Dou, Z. Li, P. Lin, Y. Wei, Y. Chen, W. Cao and H. He, "An improved prediction model of vortex shedding noise from blades of fans," *Journal of Thermal Science,* vol. 25, no. 6, pp. 526-531, 2016.

[8] C. Lee, M. K. Chung and Y. H. Kim, "A prediction model for the vortex shedding noise from the wake of an airfoil or axial flow fan blades," *Journal of Sound and Vibration,* vol. 164, no. 2, pp. 327-336, 1993.

[9] A. S. Hersh, P. T. Sodermant and R. E. Hayden, "Investigation of acoustic effects of leading-edge serrations on airfoils," *Journal of Aircraft,* vol. 11, no. 4, pp. 197-202, 1974.

[10] A. Fathy, M. I. Rashed and E. Lumsdaine, "A theoretical investigation of laminar wakes behind airfoils and the resulting noise pattern," *Journal of Sound and Vibration,* vol. 50, no. 1, pp. 133-144, 1977.

[11] M. R. Fink, "Prediction of airfoil tone frequencies," *Journal of Aircraft,* vol. 12, no. 2, pp. 118-120, 1975.

[12] "Regulation of the EC (EU) No. 327/2011, of 30. 03. 2011, implementing Directive 2009/125/EC of the EP and of the Council of the EU with regard to ecodesign requirements for fans driven by motors with an electric input power between 125 W and 500 kW," *Official Journal of the European Union,* p. 8–21, 6 April 2011.

[13] F. V. Hutcheson and T. F. Brook, "Effects of angle of attack and velocity on trailing edge noise determined using microphone array measurements," *International Journal of Aeroacoustics,* vol. 5, no. 1, pp. 39-66, 2006.

[14] T. Geyer, E. Sarradj and J. Giesler, "Application of a Beamforming Technique to the Measurement of Airfoil Leading Edge Noise," *Advances in Acoustics and Vibration,* Vols. 2012, Article ID 905461, p. 16, 2012.

[15] D. J. Moreau and C. J. Doolan, "Tonal noise production from a wall-mounted finite airfoil," *Journal of Sound and Vibration,* vol. 363, pp. 199-224, 2016.

[16] P. Migliore and S. Oerlemans, "Wind tunnel aeroacoustic tests of six airfoils for use on small wind turbines," *Journal of Solar Energy Engineering,* vol. 126, no. 4, pp. 974-985, 2004.

[17] D. J. Moreau, Z. Prime, R. Porteous, C. J. Doolan and V. Valeau, "Flow-induced noise of a wall-mounted finite airfoil at low-to-moderate Reynolds number," *Journal of Sound and Vibration,* vol. 333, no. 25, pp. 6924-6941, 2014.

[18] S. Yarusevych, P. E. Sullivan and J. G. Kawall, "On vortex shedding from an airfoil in low-Reynolds-number flows," *Journal of Fluid Mechanics,* vol. 632, pp. 245-271, 2009.